Original Research

Periodic heart rate decelerations in premature infants

Abigail A Flower[1], J Randall Moorman[2], Douglas E Lake[2] and John B Delos[3]

[1]Structural, Computational Biology and Biophysics Program; [2]Department of Internal Medicine, Cardiovascular Division, University of Virginia, Charlottesville, VA 22903; [3]Department of Physics, College of William and Mary, PO Box 8795, Williamsburg, VA 23187-8795, USA

Corresponding author: John B Delos. Emails: jbdelo@wm.edu, jbdelos@cox.net

Abstract

The pacemaking system of the heart is complex; a healthy heart constantly integrates and responds to extracardiac signals, resulting in highly complex heart rate patterns with a great deal of variability. In the laboratory and in some pathological or age-related states, however, dynamics can show reduced complexity that is more readily described and modeled. Reduced heart rate complexity has both clinical and dynamical significance – it may provide warning of impending illness or clues about the dynamics of the heart's pacemaking system. In this paper, we describe simple and interesting heart rate dynamics that we have observed in premature human infants – reversible transitions to large-amplitude periodic oscillations – and we show that the appearance and disappearance of these periodic oscillations can be described by a simple mathematical model, a Hopf bifurcation.

Keywords: heart rate variability, neonatal, Hopf bifurcation

Experimental Biology and Medicine 2010; **235**: 531–538. DOI: 10.1258/ebm.2010.009336

Introduction

The normal, healthy heart beats at a variable rate with extraordinarily complex fluctuations across a wide range of timescales.[1–9] This phenomenon is commonly referred to as heart rate variability (HRV). Multiple mechanisms contribute to HRV; it is a composite reflection of autonomic outflow (the combination of sympathetic and parasympathetic nervous system activation), neuroendocrine influences and autonomic responsiveness (the ability of the cardiovascular system to respond to changes in autonomic outflow).[2] It has been demonstrated that this healthy complex variability deteriorates as a consequence of disease and aging.[1,2,5,7] Complexity in HR may be easy to see but it is hard to define, so there are many different measures of complexity, having varying degrees of utility in different contexts.[10–22]

Regularity, on the other hand, is often easy to see and easy to define precisely, especially when that regularity has the form of periodic cycles. Two periodic cycles of HR have been extensively studied. Respiratory sinus arrhythmia, the coupling of HR to breathing, produces fluctuations in HR with a period of a few seconds in adults or about one second in infants in a neonatal intensive care unit (NICU).[23,24] Another cycle of HR is correlated with a cycle of blood pressure called Mayer waves;[25,26] the period of these is about 10 s in adults or 12–14 s in NICU patients.[23] In these infants, who typically have interbeat intervals near 350 ms (and HR around 170 beats per minute), the magnitude of the changes of interbeat intervals due to respiratory sinus arrhythmia is about 2–4 ms, while that associated with Mayer waves is about 10 ms. Combined they can sum to give periodic fluctuations of magnitude around 5% of the interbeat interval. Other lower frequency components elevate the range of fluctuations of HRs further,[6] but these are less cyclical.

We describe here in infants a different and previously uncharacterized HR cycle with large decelerations. A deceleration is a decrease in HR followed by a return to the base rate. In previous work, we have found that HR decelerations in the setting of otherwise low HRV often preceded acute neonatal illness such as sepsis, a severe bacterial infection of the bloodstream.[27–33] In those studies, we used statistical measures based on HR distributions to make predictive models for clinical use.

For this new work, we devised a wavelet-based detector of decelerations in HR records and applied it to a large clinical database. We find that large decelerations are similar in shape among infants, and can appear in clusters in which they are sometimes remarkably periodic for epochs as long as two days. These cycles do not resemble any well-characterized HR oscillation, and we propose that they constitute a previously unrecognized form of low-dimensional HR dynamics. We tested the hypothesis

that clusters of periodic decelerations might result from a Hopf bifurcation, a common way for a steady state to change to a cycle.

Methods

Patient population

We studied the HR records of 479 very low birth weight (<1500 g) neonates from NICUs at the University of Virginia, the University of Alabama at Birmingham and Wake Forest University, with a total of 513,193 half-hour HR records. We extracted interbeat (RR) intervals as described previously.[27,28,31–33] The rhythm was presumed to be sinus in all cases, as QRS complexes were consistently preceded by P waves with no variations in their morphology.

A neonatal HR deceleration detector

To investigate the dynamics, we developed a neonatal HR deceleration detector using a pattern-matching algorithm inspired by wavelet theory.[34] We defined a template function that gives an adequate description of the shape of a deceleration, and swept this function through the RR interval time series to identify points at which the HR signal matched the template within a specified tolerance.

To employ this scheme effectively, an appropriate template function, χ, was needed. Consider, for example, panel (d) of Figure 1, in which repeated decelerations appear. Figure 2a shows several decelerations from the record shown in Figure 1d superimposed atop one another. To the eye, the decelerations are relatively symmetric in shape and, compared with a Gaussian, are narrower at the peak and wider in the wings. A function that meets these criteria and subsequently has proven to successfully locate decelerations of similar nature throughout signals from many infants is as follows:

$$\chi_b(n-n_0) = \exp\left(-g(s)\right), \quad -4 \le s \le 4,$$
$$g(s) = \frac{s^2}{1+|s|^{3/2}}, \tag{1}$$
$$s = (n-n_0)/b,$$

where b is a width parameter and n_0 is a translation parameter. The goodness of fit of this function was high; when compared with visually identified decelerations, the median R-squared value was 0.93. In addition, this $\chi_b(n-n_0)$ function consistently provided a reasonable estimate of the height of a deceleration relative to its baseline. Thus, $\chi_b(n-n_0)$ was used as a template for a deceleration detector. We do not attach any theoretical significance to this function; rather, it has been reached empirically as a function that represents the shape of typical decelerations.

To detect decelerations in the signals that also contain fluctuations associated with normal HRV, we treated the RR interval (time interval between beats) signal as if it were a sum of that deceleration function plus some remainder:

$$RR(n) = a\chi_b(n-n_0) + G(n)\ . \tag{2}$$

Here $RR(n)$ is the time between beat n and beat $n+1$, $\chi_b(n-n_0)$ is the function describing a deceleration of width b centered about the point n_0 and $G(n)$ is the remainder of the signal (Figure 3). The value a represents the height or amplitude of the deceleration; it is estimated by finding local maxima of the function

$$a(n_0,b) = \frac{\overline{RR\chi_b}}{\overline{\chi_b^2}}. \tag{3}$$

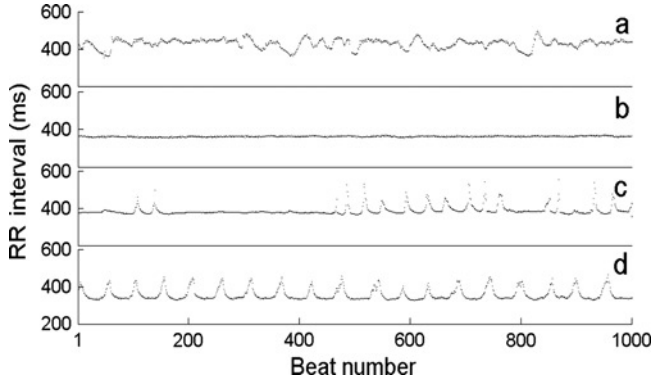

Figure 1 Examples of approximately four minutes of continuous RR (interbeat) intervals from four different NICU patients. (a) RR interval series for a healthy NICU patient; (b) RR interval series for an NICU patient showing reduced heart rate variability prior to diagnosis of sepsis (bloodstream infection); (c) RR interval series for an NICU patient showing decelerations; and (d) RR interval series showing part of a long cluster of periodic decelerations. Each peaked structure in (c) and (d) is termed a 'deceleration.' (d) Striking periodicity (period ~45 beats, or about 15 s), which lasted well beyond the duration of the shown excerpt; the periodic decelerations lasted over 48 h. (This infant suffered intracranial hemorrhage with concomitant sepsis.). NICU, neonatal intensive care unit

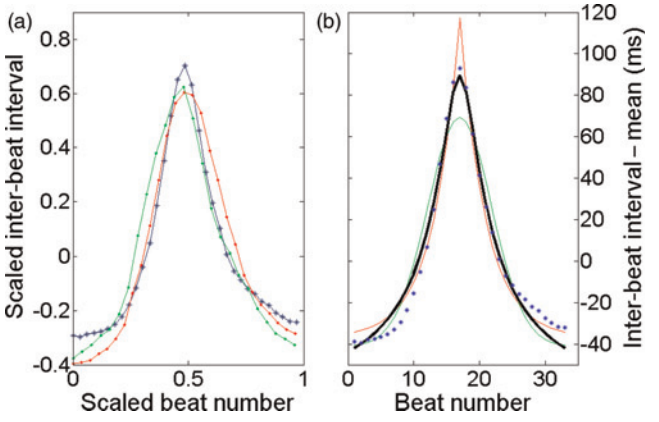

Figure 2 Decelerations have a common shape that can be represented by a template function for use in a deceleration detector. (a) Three decelerations from a record scaled to width of one and height of one. (b) Standard functions are optimized to fit a deceleration: blue asterisks, data; red line, exponential; green line, Gaussian; black line, χ. A Gaussian function is too rounded, while an exponential is too sharply peaked, but χ fits the data adequately (A color version of this figure is available in the online journal)

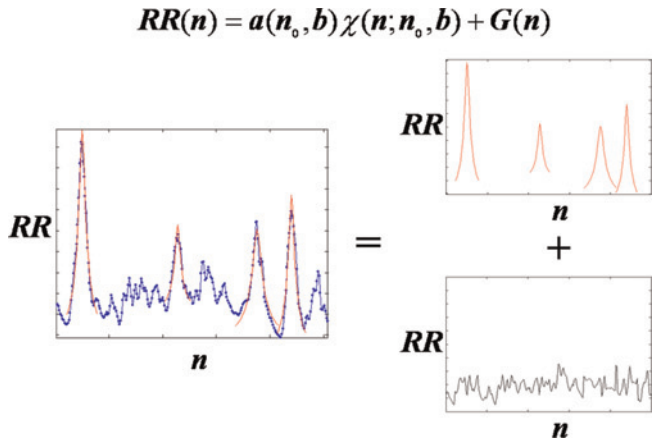

Figure 3 A typical decomposition of RR interval (interbeat interval) signal into a sum of decelerations of various widths and heights and some remainder. The red curves represent the functions $a\chi_b$ $(n - n_0)$. *a* describes the height of the function, n_0 represents the location of the peak of the function and *b* represents the width (or scale) of the function. *G*(*n*), the remaining signal after decelerations are removed, is represented in black (A color version of this figure is available in the online journal)

The numerator $\overline{RR\chi_b}$ is the projection of a portion of the signal $RR(n)$ onto the waveform of the deceleration:

$$\overline{RR\chi_b} = \sum_{n=n_0-N}^{n_0+N} RR(n)\chi_b(n - n_0), \qquad (4)$$

where N is defined consistently with $|s| \leq 4$ in Equation (1). If the remainder $G(n)$ from Equation (2) has the properties of Gaussian white noise, then Equation (3) is the maximum-likelihood estimate of a.

We swept this template function $\chi_b(n - n_0)$ through the signal $RR(n)$ and calculated the correlation coefficient $a(n_0, b)$ at each width b ranging from eight beats to 100 beats, and at each translation. This process generated a surface of $a(n_0, b)$ values like that shown in Figure 4. We then found the points (n_0, b) at which $a(n_0, b)$ had a local maximum, that is, where the correlation between the deceleration waveform and the signal was strongest. Having isolated these (n_0, b) points, we added several more stipulations in order to identify decelerations. First, if there were more than one local maximum near a particular translation, we picked the largest of the maxima (highest coefficient a) so that one deceleration was not erroneously represented by two waveforms. Next, to avoid spurious correlations, we required that the wavelet $a\chi_b(n - n_0)$ fit the original signal with an R-squared value of at least 0.75. For each such deceleration, the corresponding maximum value of $a(n_0, b)$ was used in Equation (2) to represent the amplitude of the deceleration.

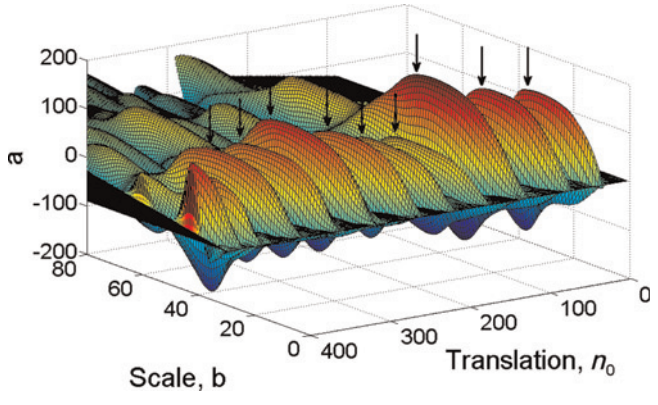

Figure 4 $a(n_0, b)$ for a portion of neonatal heart rate data. We identify the large local maxima of the surface as decelerations (indicated by black arrows). The surface $a(n_0, b)$ was generated by sweeping the template function, $\chi(n_0, b)$, through a portion of neonatal HR data at various widths (or scales), *b* (A color version of this figure is available in the online journal)

Results

Overview: normal and abnormal neonatal HR characteristics

Some examples of neonatal RR interval time series are shown in Figure 1. Panel (a) is a complex time series of a healthy NICU infant; panel (b) is a time series showing reduced variability of an NICU infant with sepsis; panel (c) is a time series with decelerations (each spike in the RR interval time series is a deceleration, or a slowing of the HR followed by return to a base rate); and panel (d) is a time series with periodic decelerations. Compared with case (a), case (d) plainly represents reduced-dimensional dynamics. In this example, which was drawn from an infant with intracerebral hemorrhage and sepsis, the period of the decelerations is nearly constant at about 45 beats, or 15 seconds, and, while the decelerations have a variety of heights (which can be anywhere from 20 to 300 ms), they have a common shape.

Automated detection and analysis of neonatal HR decelerations

Figure 2a shows several superimposed decelerations from this infant, and emphasizes the similarity of the time courses. Figure 2b shows the fit to several candidate templates – the function χ (n) is shown in black, and fits the data in blue points better than Gaussian or exponential functions. Figure 3 shows an example of the automated detection scheme. The RR interval time series was analyzed for decelerations that were fit well by $\chi_b(n - n_0)$, and each was characterized by its parameters: height a, width b and location n_0. The residual signal might then be analyzed separately for its statistical properties. Figure 4 gives further details of the wavelet-based aspects of the detection scheme. The plot shows $a(n_0, b)$ for a short RR interval time series. The x- and y-axis are the width parameter b and the location parameter n_0, and the z-axis is the correlation coefficient $a(n_0, b)$. In this short time series, there are multiple large decelerations that are fit well by $\chi_b(n - n_0)$; these are marked with arrows. The height parameter a for each deceleration is the local maximum of $a(n_0, b)$. For the analysis that follows, we focused on decelerations that were at least 100 ms in height, although there is clearly a continuum of heights of distinct decelerations.

Decelerations were isolated or occurred in clusters

We found that tall decelerations were usually isolated or, less commonly, occurred in clusters lasting up to two days. Figure 5a shows a half-hour excerpt of such a cluster, the whole of which lasted approximately one day late in the hospital course and was associated with an episode of neonatal sepsis (Figure 5b). Within such extended clusters of decelerations, we sometimes found shorter intervals of time, lasting up to several hours, in which the decelerations showed remarkable periodicity (Figure 5c). These periodic sequences of decelerations lasting 10 min or more without interruption were rare; they were seen in six cases out of the population of several hundred patients. Remarkably, in each case the period of decelerations was about 15 s (Figure 5d).

Tall decelerations were common: at least one occurred in about 1/3 of our 20–30 min records. Most were isolated – only about one per 1000 records had four or more decelerations. Many but not all cases occurred near the time of neonatal sepsis, and a more complete clinical description will appear elsewhere.

Dynamical interpretation: Hopf bifurcations of neonatal HR

A cluster of periodic decelerations having a common shape suggests low-dimensional dynamics. Moreover, the clusters began and ended abruptly. Interestingly, small amplitude oscillations of similar period were often present in the vicinity of these clusters (Figures 5c and 6c). All of these behaviors are consistent with a Hopf bifurcation in a noisy system; in fact, a Hopf bifurcation is the most general way a system can change from stable to oscillatory. Such bifurcations occur, for example, in laser systems, oscillatory chemical reactions, predator–prey dynamics and in the Hodgkin–Huxley model of the squid giant axon.[35–39] The effect of noise on a system having a Hopf bifurcation was described by Wiesenfeld and his collaborators.[40,41]

The theory of Hopf bifurcations is well known, and we summarize just enough of it in the Appendix to show how we do our simulations. Neonatal HR is assumed to be under the control of multiple dynamical processes described by differential equations. Hopf theory reduces a large set of differential equations containing many parameters to one pair of differential equations with one governing parameter. If the parameter (called μ) varies slowly with time near a pair of critical values, then the HR changes between small fluctuations and large periodic oscillations.

Using this model (see the Appendix), it is possible to simulate on a computer clusters of periodic decelerations similar to those observed in the clinical data (Figure 6). Furthermore, by specifying the times at which decelerations begin and end, and forcing the parameter μ to cross its critical points accordingly, one can reasonably capture the essential elements of the HR data, including the noisy precursors, abrupt starts and stops and repeating cycles of decelerations (Figure 6c).

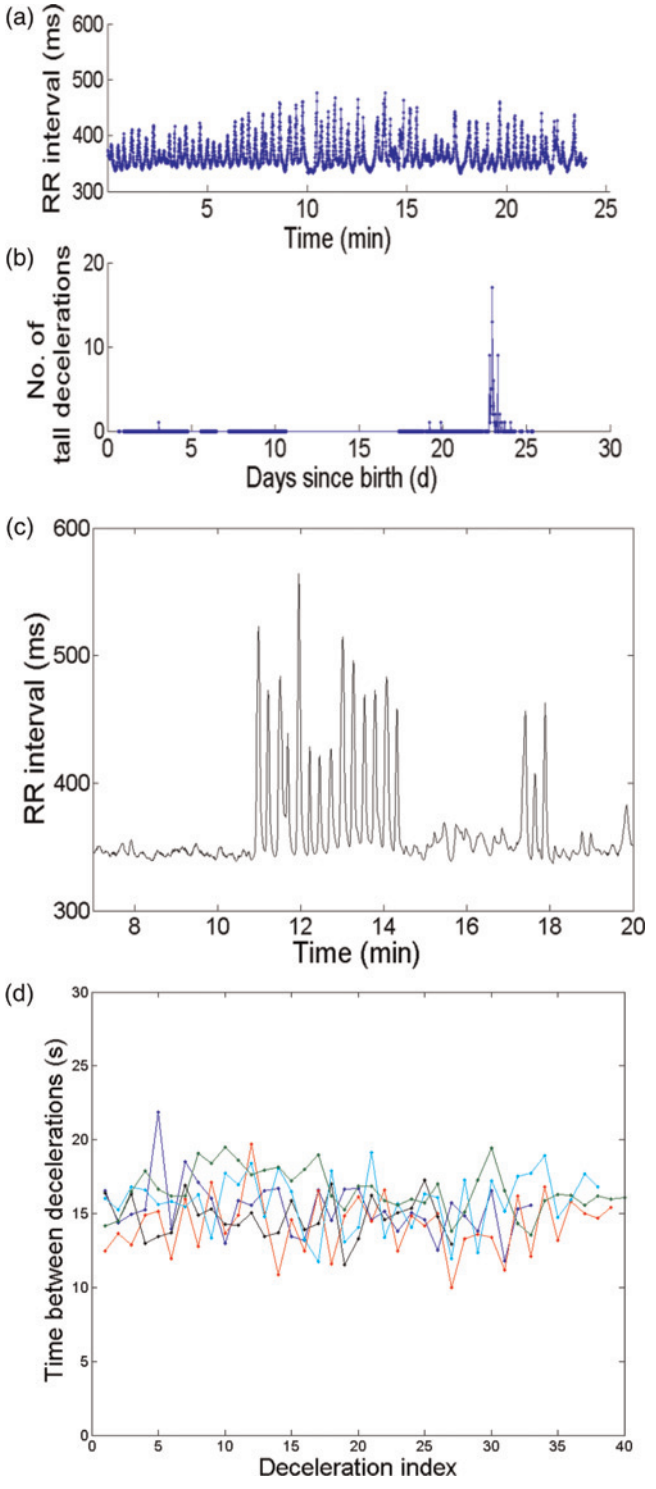

Figure 5 Decelerations occur in clusters that may show periodicity. (a) Example of a cluster of tall decelerations in a half-hour record of RR. (b) For the same infant, number of tall decelerations (greater than 100 ms from peak to baseline) in a half-hour record as a function of days since birth. Each data point represents one half-hour record. Through most of the infant's stay, there were few occurrences of tall decelerations, but a cluster occurred around day 23. (Six hours later, this patient showed clinical signs of sepsis.) (a) A record from the cluster occurring near day 23. Note the presence of intermittent periodicity in (a). (c) A burst of decelerations arising from a state of low variability. The abrupt onset of the decelerations is indicative of a 'hard' Hopf bifurcation. (d) Periodic bursts of decelerations for six NICU infants. We show time to next deceleration as a function of deceleration index. The typical time between decelerations is about 15 s. NICU, neonatal intensive care unit (A color version of this figure is available in the online journal)

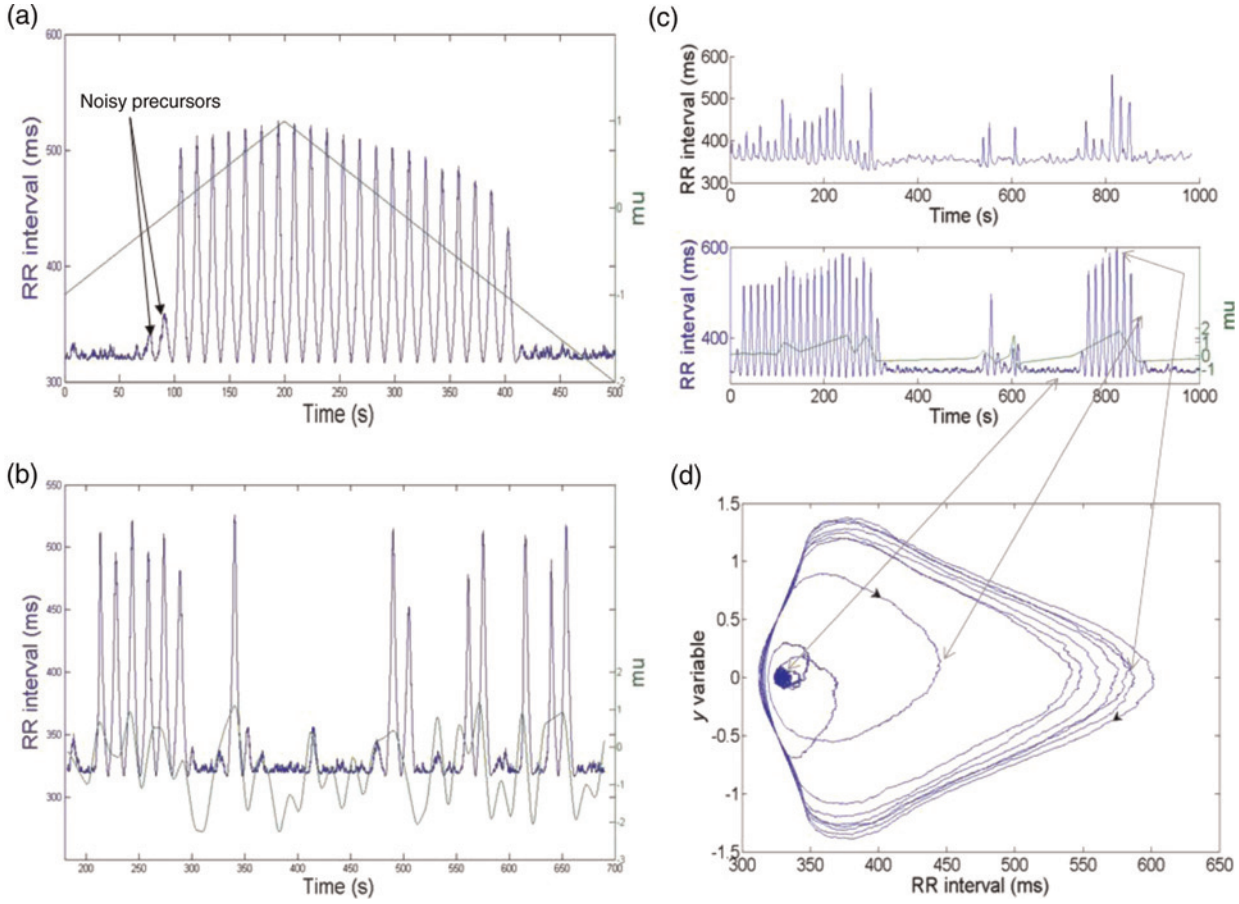

Figure 6 A Hopf bifurcation model with noise produces behavior similar to that of observed data. (a) Simulated behavior of RR intervals showing a transition from small fluctuations to noisy precursors to large oscillations. Oscillations arise when μ increases through zero, and terminate when μ decreases through its critical value, in this case -1 (μ plotted in green, RR intervals in blue). (b) Bursts of periodic decelerations created by allowing the parameter μ to vary near zero. Such results of simulations resemble observed data. (c) (Top) Data from a neonatal RR interval record showing bursts of periodic decelerations. (Bottom) Simulation of data produced by the noisy Hopf model. (d) A portion of the same simulation shown in coordinates (*RR*, *y*). The noisy precursors have $RR \sim 335$, $y \sim 0$. When μ increases through zero, that point becomes unstable, and the path quickly spirals out to a large cycle. When μ decreases through its critical point again, the path spirals back to fluctuate again about the now-stable steady state (A color version of this figure is available in the online journal)

Another way to show the cycle is in Cartesian coordinates $(x, y) = (r \cos \theta, r \sin \theta)$ or, better, in coordinates (RR, y). Part of the simulation shown in Figure 6c is shown in these variables in Figure 6d.

Discussion

Using a new wavelet-based deceleration detector, we have described an apparently new type of periodic behavior in the HRs of neonates. Their period is nearly constant at about 15 s, and their sizes may increase the interbeat interval from 350 to 550 ms or reduce the HR from 170 to 110 beats per minute. Thus, these cycles of decelerations are much too long and much too large to represent respiratory sinus arrhythmia, and, although the period is comparable, they are much larger than reported Mayer waves in infants,[23] up to 10 times larger in amplitude than are seen in those cases. We have interpreted the behavior as a Hopf bifurcation in a noisy system, and we have found that this two-dimensional dynamical model, based on minimal assumptions, gives a credible simulation of periodic neonatal HR decelerations. If this interpretation is correct, then we are reporting here for the first time the observation of a previously unknown bifurcation in the dynamics of the control system of the human HR.

We recognize several limitations of this analysis. First, we do not know the physiological mechanism of the decelerations. We have speculated that cytokine release as a response to infection or other insult might alter signal transduction in the sinus node; alternatively, cytokines might affect the control loops connecting HR to respiration, O_2 saturation and blood pressure. Second, we do not yet know all the clinical correlates or ramifications of repeated decelerations; we will elsewhere make a more complete report. Third, we recognize that the good results of modeling and simulation using Hopf bifurcation theory do not mean that these are the only possible dynamics. The idea of low-dimensional dynamics fits with current concepts of reduced complexity of HR during illness, and this Hopf model is a good candidate for description of the observations.

This phenomenon of periodically repeated decelerations is interesting from both dynamical and clinical perspectives. It is dynamically interesting because it shows that the immature control system of the HR can go into a previously uncharacterized oscillatory mode. These observations

therefore can provide a new point of contact with mathematical models of the control system.[42–44]

The clinical significance of this phenomenon is not completely known. There is no doubt about the statistical association of decelerations with neonatal sepsis; i.e. those infants with frequent HR decelerations are more likely than the average infant to be diagnosed with sepsis in the next 24 h. However, several infants with frequent decelerations appeared to be healthy, and no clinical diagnosis of sepsis was made. One possibility is that there was subclinical infection that resolved on its own, another is subclinical intracerebral hemorrhage and still another is episodic neonatal apnea. Since long periodic sequences of decelerations occurred spontaneously in the clinical setting and were not induced by controlled means, they must be a normal or pathological mode of low-dimensional dynamics in the human cardiac pacemaking system near the time of birth.

Author contributions: All authors participated in the analysis and interpretation of data and review of the manuscript.

ACKNOWLEDGEMENTS

This work was supported by NIGMS 64640. AAF was supported by National Heart, Lung and Blood Institute Basic Cardiovascular Research Training Grant 5T32-HL-07284. JBD is supported by NSF Grant PHY-0457070. Computing support was provided by the SciClone Cluster Project at the College of William and Mary. We thank Dr Gene Tracy for his helpful suggestions.

Conflict of interest: Medical Predictive Science Corporation of Charlottesville, VA, has a license to market technology related to heart rate characteristics monitoring of newborn infants, supplied partial funding for this study and aided in collection of data. They played no role in study design, analysis and interpretation of data, or of the writing of the report or the decision to submit the paper for publication. Drs Lake and Moorman have an equity share in this company.

REFERENCES

1 Buchman TG. Nonlinear dynamics, complex systems, and the pathobiology of critical illness. *Curr Opin Crit Care* 2004;**10**:378
2 Buchman TG, Stein PK, Goldstein B. Heart rate variability in critical illness and critical care. *Curr Opin Crit Care* 2002;**8**:311
3 Glass L, Shrier A, Belair J. Chaotic cardiac rhythms. *Chaos* 1986:236–56
4 Goldberger AL. Chaos and fractals in human physiology. *Sci Am* 1990;**262**:42–9
5 Goldberger AL, Peng C-K, Lipsitz LA. What is physiologic complexity and how does it change with aging and disease? *Neurobiol Aging* 2002;**23**:23–6
6 Goldberger AL. Heartbeats, hormones, and health is variability the spice of life? *Am J Respir Crit Care Med* 2001;**163**:1289–90
7 Goldberger AL, Amaral LAN, Hausdorff JM, Ivanov PC, Peng CK, Stanley HE. Fractal dynamics in physiology: alterations with disease and aging. *Proc Natl Acad Sci* 2002;**99**:2466–72
8 Guevara MR, Glass L, Shrier A. Phase locking, period-doubling bifurcations, and irregular dynamics in periodically stimulated cardiac cells. *Science* 1981;**214**:1350–3
9 Ivanov PC, Rosenblum MG, Peng C, Mietus J, Havlin S, Stanley HE, Goldberger AL. Scaling behaviour of heartbeat intervals obtained by wavelet-based time-series analysis. *Nature* 1996;**383**:323–7
10 Badii R, Politi R. Complexity, Heirarchical Structures and Scaling in Physics. Cambridge: Cambridge University Press, 1997
11 Ben-Jacob E. From snowflake formation to growth of bacterial colonies II: cooperative formation of complex colonial patterns. *Contemp Phys* 1997;**38**:205–41
12 Hulata E, Baruchi I, Segev R, Shapira Y, Ben-Jacob E. Self-regulated complexity in cultured neuronal networks. *Phys Rev Lett* 2004;**92**:198105
13 Costa M, Healy J. Multiscale entropy analysis of complex heart rate dynamics: discrimination of age and heart failure effects. *Comput Cardiol* 2003:705–8
14 Goldenfeld N, Kadanoff LP. Simple lessons from complexity. *Science* 1999;**284**:87–9
15 Kotani K, Takamasu K, Ashkenazy Y, Stanley HE, Yamamoto Y. Model for cardiorespiratory synchronization in humans. *Phys Rev E* 2002;**65**:51923
16 Lee UC, Kim S, Yi S. Event and time-scale characteristics of heart-rate dynamics. *Phys Rev E* 2005;**71**:61917
17 Li J, Ning X. Dynamical complexity detection in short-term physiological series using base-scale entropy. *Phys Rev E* 2006;**73**:52902
18 Lin D. Robustness and perturbation in the modeled cascade heart rate variability. *Phys Rev E* 2003;**67**:31914
19 Marwan N, Wessel N, Meyerfeldt U, Schirdewan A, Kurths J. Recurrence-plot-based measures of complexity and their application to heart-rate-variability data. *Phys Rev E* 2002;**66**:26702
20 Raab C, Wessel N, Schirdewan A, Kurths J. Large-scale dimension densities for heart rate variability analysis. *Phys Rev E* 2006;**73**:41907
21 Żebrowski J, Baranowski R. Direct observation of homoclinic orbits in human heart rate variability. *Phys Rev E* 2003;**67**:56216
22 Glass L. Introduction to controversial topics in nonlinear science: Is the normal heart rate chaotic? *Chaos: An Interdisciplinary Journal of Nonlinear Sciences* 2009;**19**:028501
23 Andriessen P, Koolen AMP, Berendsen RCM, Wijn PFF, Ten Broeke EDM, Oei SG, Blanco CE. Cardiovascular fluctuations and transfer function analysis in stable preterm infants. *Pediatr Res* 2003;**53**:89
24 Andriessen P, Schoffelen RLM, Berendsen RCM, Am De Beer N, Oei Sg, Wijn PFF, Blanco CE. Noninvasive assessment of blood pressure variability in preterm infants. *Pediatr Res* 2004;**55**:220
25 Mayer S. Studien zur physiologie des herzens und der blutgefasse. *Sitz Kaiser Akad Wiss* 1876;**74**:281
26 Julien C. The enigma of Mayer waves: facts and models. *Cardiovasc Res* 2006;**70**:12
27 Griffin MP, Moorman JR. Toward the early diagnosis of neonatal sepsis and sepsis-like illness using novel heart rate analysis. *Pediatrics* 2001;**107**:97–104
28 Griffin MP, O'Shea TM, Bissonette EA, Harrell FE, Lake DE, Moorman JR. Abnormal heart rate characteristics preceding neonatal sepsis and sepsis-like illness. *Pediatr Res* 2003;**53**:920–6
29 Griffin MP, Lake DE, Bissonette EA, Harrell FE, O'Shea TM, Moorman JR. Heart rate characteristics: novel physiomarkers to predict neonatal infection and death. *Pediatrics* 2005;**116**:1070–4
30 Griffin MP, Lake DE, Moorman JR. Heart rate characteristics and laboratory tests in neonatal sepsis. *Pediatrics* 2005;**115**:937–41
31 Griffin MP, Lake DE, O'Shea TM, Moorman JR. Heart rate characteristics and clinical signs in neonatal sepsis. *Pediatr Res* 2007;**61**:222
32 Lake DE, Griffin MP, Moorman JR. New mathematical thinking about fetal heart rate characteristics. *Pediatr Res* 2003;**53**:889–90
33 Moorman J, Lake D, Griffin M. Heart rate characteristics monitoring for neonatal sepsis. *IEEE Trans Biomed Eng* 2006;**53**:126–32
34 Kaiser G. *A Friendly Guide to Wavelets*. Boston: Birkhäuser, 1994
35 Fussmann GF, Ellner SP, Shertzer KW, Hairston NG Jr. Crossing the hopf bifurcation in a live predator–prey system. *Science* 2000;**290**:1358–60
36 Xie Y, Chen L, Kang YM, Aihara K. Controlling the onset of hopf bifurcation in the Hodgkin–Huxley model. *Phys Rev E* 2008;**77**:61921
37 Marsden JE, McCracken M, Chernoff P. The Hopf Bifurcation and its Applications. New York: Springer, 1976
38 Guckenheimer J, Holmes P. *Nonlinear Oscillations, Dynamical Systems, and Bifurcations of Vector Fields*. New York: Springer-Verlag, 1983
39 Arnold VI. *Geometrical Methods in the Theory of Ordinary Differential Equations*. New York: Springer, 1988
40 Jeffries C, Wiesenfeld K. Observation of noisy precursors of dynamical instabilities. *Phys Rev A* 1985;**31**:1077–84

41 Wiesenfeld K. Virtual hopf phenomenon: a new precursor of period-doubling bifurcations. *Phys Rev A* 1985;**32**:1744–51
42 de Boer R, Karemaker J, Strakee J. Hemodynamic fluctuations and baroreflex sensitivity in humans: a beat-to-beat model. *Am J Physiol – Heart Circ Physiol* 1987;**253**:H680–H689
43 Ottesen JT. Modelling of the baroreflex – feedback mechanism with time-delay. *J Math Biol* 1997;**36**:41–63
44 Seidel H, Herzel H. Modeling heart rate variability due to respiration and baroreflex. In: Mosekilde E, Mouritsen OG, eds. *Modeling the Dynamics of Biological Systems.* Berlin: Springer, 1995:205–29

(Received October 21, 2009, Accepted February 1, 2010)

Appendix: Hopf bifurcation analysis of neonatal HR decelerations

One assumes that the pacemaking system of the heart has feedback loops that can be modeled by a large number of dynamical variables (denoted $\mathbf{u} = [u_1 \ldots u_n]$) governed by an equally large number of differential equations,

$$\frac{d\mathbf{u}}{dt} = f(\mathbf{u};\mathbf{p}). \tag{A.1}$$

These governing equations are assumed to contain many parameters $\mathbf{p} = p_1 \ldots p_m$, which may vary with time in the following way: on short timescales, they may have small, rapid, noisy fluctuations but generally they do not have large changes; on long timescales, they have substantial slow variation. (In our case, timescales are 'short' or 'long' compared with the duration of typical decelerations, about 15 s.) The functions, $f(\mathbf{u};\mathbf{p})$, governing the rate of change of $\mathbf{u}$ are not presumed to be known. However, it is assumed that these functions have Taylor expansions that converge in the range of interest, and that these functions have a zero (steady state), which can be taken to occur at $\mathbf{u} = 0$. For some values of the parameters $\mathbf{p}$, the steady state is assumed to be stable.

The first step is linear stability analysis. If the Taylor expansions are truncated at first degree, one obtains a set of linear equations:

$$\frac{d\mathbf{u}}{dt} = \mathbf{M}(\mathbf{p})\mathbf{u}. \tag{A.2}$$

The eigenvalues of the matrix $\mathbf{M}(\mathbf{p})$ associated with these linear equations must either be real or occur in complex–conjugate pairs. When all real parts of these eigenvalues are negative, the steady state is stable. The steady state can go unstable if, as the parameters $\mathbf{p}$ change, one real eigenvalue, or a pair of complex–conjugate eigenvalues, crosses the imaginary axis. Hopf theory examines the latter case and provides two powerful theorems. (1) 'Center Manifold Theorem': In the state space of dynamical variables $\mathbf{u}$, there is a two-dimensional surface (called a center manifold), which is an invariant surface and an attractor. That means: (a) if $\mathbf{u}(t)$ lies initially on this two-dimensional surface, it stays on this surface; (b) if $\mathbf{u}(t)$ lies initially off the surface, it moves toward the surface in the manner of exponential decay. Furthermore, the surface is analytic (Taylor expandable) and the evolution in the surface can be described by two differential equations. (2) 'Normal Form Theorem': There exists an analytic change of variables to new coordinates (x, y) such that the governing pair of equations can be reduced to a standard 'normal' form:

$$\begin{aligned}\frac{dx}{dt} &= -\mu x - \omega y - \hat{c}(y^3 + yx^2) + \hat{a}(x^3 + xy^2) \\ &\quad - \hat{d}(y^5 + 2x^2y^3 + yx^4) + \hat{b}(x^5 + 2x^3y^2 + xy^4), \\ \frac{dy}{dt} &= -\mu y + \omega x + \hat{c}(x^3 + xy^2) + \hat{a}(y^3 + yx^2) \\ &\quad + \hat{d}(x^5 + 2x^3y^2 + xy^4) + \hat{b}(y^5 + 2x^2y^3 + yx^4).\end{aligned} \tag{A.3}$$

In polar coordinates, that normal form is

$$\begin{aligned}\frac{dr}{dt} &= \mu r + \hat{a}r^3 + \hat{b}r^5 + \cdots \\ \frac{d\theta}{dt} &= \omega + \hat{c}r^2 + \hat{d}r^4 + \cdots\end{aligned}. \tag{A.4}$$

The new parameters μ, $\hat{a} \ldots \hat{d}$ and ω depend on the parameters $\mathbf{p}$. If, as the parameters $\mathbf{p}$ vary with time, μ changes from negative to positive, the stable steady state goes unstable, and one of two things happens: (1) if $\hat{a} < 0$, a stable cycle is created (this is a 'soft' Hopf bifurcation, also called 'supercritical'); (2) if $\hat{a} > 0$, an unstable cycle is destroyed; in this case, if $\hat{b} < 0$, the radius $r(t)$ can go quickly to a large value while the angle θ (t) increases steadily, so the system 'jumps' to a large cycle of frequency ω (this is a 'hard' Hopf bifurcation, also called 'subcritical').

To generate simulations, we integrated Equation (A.3), adding random noise to both variables after every time step, Δt. This noise term was multiplied by a coefficient, $\varepsilon = \xi\sqrt{\Delta t}$. The factor ξ controls the strength of the noise and, for our simulations, generally assumed a value between 0.01 and 0.1. The factor $\sqrt{\Delta t}$ ensures that the statistical properties of the noise fluctuations are independent of the step size Δt (the width parameter of the distribution resulting from a random walk is proportional to the size of each step times the square root of the number of steps). The integration was carried out for various values of parameters μ, $\hat{a}$ and $\hat{b}$. The parameter $\hat{a}$ was always kept positive and $\hat{b}$ negative in order to keep the bifurcation 'hard'; $\hat{c}$ and $\hat{d}$ were set to zero, because we have no clear evidence that the frequency of periodic decelerations varies systematically with their height. For cases in which parameters fluctuated in time, we set μ initially negative, and allowed it to vary near zero.

If μ is constant and positive, then $x(t)$ and $y(t)$ have perfectly sinusoidal oscillations. If μ varies slowly while remaining positive, then the amplitude of the oscillations, and hypothetically also the frequency, also vary slowly. If μ is fixed just below zero, and the initial values of $x(t)$ and $y(t)$ are close to zero, then in the absence of noise, $x(t)$ and $y(t)$ both approach zero exponentially. In the presence of noise, small periodic fluctuations with angular frequency near ω appear. These are called 'noisy precursors' of the large oscillations that are present for $\mu > 0$.

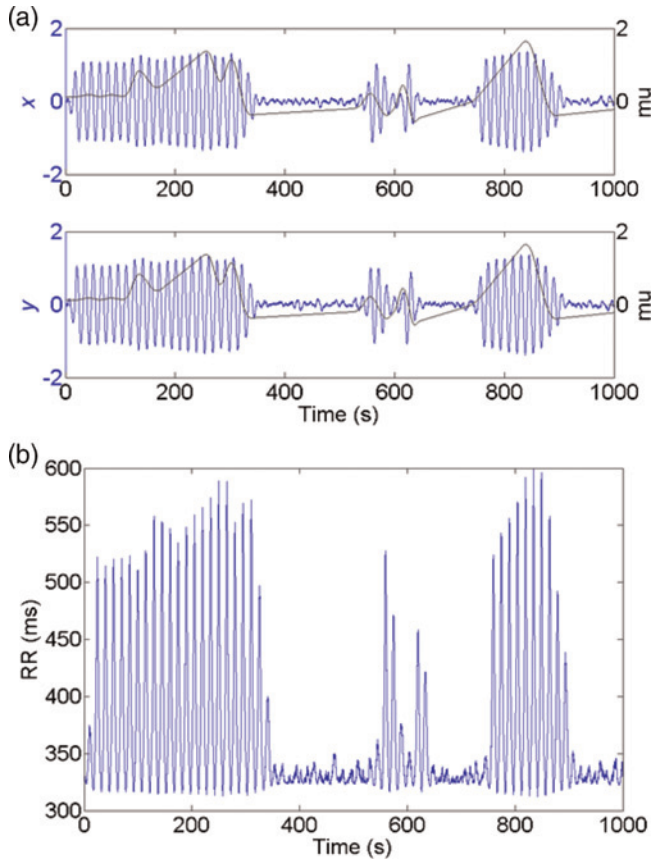

Figure 7 (a) Output from a hard Hopf model with noise coefficient, ξ, equal to 0.03, μ varying in time as shown on the plot (black line), $\hat{a} = 1/3$ and $\hat{b} = -1/2$. (Top) Variable *x* as a function of time. (Bottom) Variable *y* as a function of time. Output was produced using Equation (A.3) with the specified parameter values. (b) *RR*(*t*) corresponding to (*x*(*t*), *y*(*t*)) output of (a). *RR*(*t*) is calculated by converting the output (*x*(*t*), *y*(*t*)) of the noisy Hopf model into polar form, and then using Equation (A.5). The behavior of μ is identical to that in (a) (A color version of this figure is available in the online journal)

The behavior of the variables $x(t)$ and $y(t)$ when the parameter μ fluctuates near zero is shown in Figure 7a. As μ goes from negative to positive, $x(t)$ and $y(t)$ make transitions from low variability to noisy precursors to large oscillations. As μ subsequently decreases, the system crosses another critical point, in this case at $\mu = -1/18$, and returns to its low variability state. Hysteresis, noisy precursors and quick evolution from near-steady state to large oscillations are characteristics of hard Hopf bifurcations in systems with noise.

In Figure 7a, we have only weak resemblance to the observations. The oscillations shown there are nearly sinusoidal, and the base line is near the middle of the oscillations. We can get a respectable simulation of infant HRs if we bring in one more *postulate*: the time between beats $RR(t)$ is some function of one of these unknown variables $x(t) = r(t)\cos(\theta(t))$:

$$\begin{aligned} RR(t) &= F(x(t)) \\ &= \sum_k a_k [x(t)]^k \\ &= \sum_k a_k [r(t)]^k \cos^k \theta(t) \\ &= \sum_n c_n [r(t)]^n \cos(n\theta(t)). \end{aligned} \tag{A.5}$$

Here the presently unknown function $F(x)$ is expanded in a Taylor series and then converted to a corresponding Fourier series. But we know the shape of the decelerations – the shape is given by Equation (1). A Fourier cosine representation of that formula must agree with Equation (A.5). Taking $\theta = \pi s/4$, and $r(t) = 1$, six terms in Equation (A.5) give an accurate representation of $\chi_{b=1}(s)$ defined in Equation (1):

$$\begin{aligned} (c_0 \ldots c_5) = (&0.4428, 0.3317, 0.1103, 0.0587, \\ &0.0242, 0.0153, 0.0062). \end{aligned} \tag{A.6}$$

This transformation converts the output $x(t)$ shown in Figure 7a into a simulation of $RR(t)$ shown in Figure 7b, which resembles an RR interval time series.

The simulations shown in Figure 6 were done by the same method: choose values of $\hat{a}$ and $\hat{b}$, specify $\mu(t)$ fluctuating near zero, integrate Equations (A.3) adding noise as described above, convert $[x(t), y(t)]$ to $[r(t), \theta(t)]$, then convert to $RR(t)$ using Equations (A.5) and (A.6).